ARTICLE TYPE www.rsc.org/xxxxxx | XXXXXXXX

On the balance between syn- and anticlinicity in smectic phases formed by achiral hockey stick mesogens with and without chiral dopants

Eva Enz,[a,b] Sonja Findeisen-Tandel,[a,§] Roman Dabrowski,[c] Frank Giesselmann,[b] Wolfgang Weissflog,[a] Ute Baumeister[a] and Jan Lagerwall*[a,b]

Received (in XXX, XXX) 1st January 2007, Accepted 1st January 2007
First published on the web 1st January 2007
DOI: 10.1039/b000000x

A series of achiral hockey stick-shaped mesogens forming tilted smectic liquid crystal phases of synclinic SmC- as well as anticlinic SmC_a-type was prepared and characterized. While all homologues exhibit both phases, the balance shifts from anticlinic to synclinic order upon elongation of the terminal chain at the meta (*m*) position, defining the hockey stick shape. The elongation also leads to an increased kinetic hindrance of the transition between syn- and anticlinic phases and a decreased transition enthalpy. These observations indicate that a well-defined kink (short *m*-substituted chain) promotes the anticlinic structure while a higher flexibility between kinked and rod-shape (long *m*-substituted chain) promotes synclinic order. An intermediate chain-length homologue was selected as host material for doping with syn- and anticlinic rod-shaped chiral dopants, respectively, at varying concentrations. Opposite of what might be expected the balance between syn- and anticlinic order was not simply dictated by the choice of dopant. Instead both types of tilting order prevailed with roughly the same strength as in the achiral host regardless of which chiral material was added, up to concentrations well beyond normal doping conditions. Thus, at least with hockey stick-shaped achiral hosts, syn- as well as anticlinic chiral compounds can be used effectively as chiral dopants without necessarily having an important impact on the clinicity of the resulting mixture. The hockey stick design concept should be useful in producing achiral anticlinic-forming mesogens for low-polarization, long-pitch antiferroelectric liquid crystal mixtures. Finally, we point out that a mixture study like the one carried out here yields a conclusive means of establishing the clinicity of achiral tilted smectics, an endeavour that can sometimes be far from trivial.

Introduction

Chirality in liquid crystal phases and its relation to the structure of the constituent mesogenic molecules is a topic of considerable interest in liquid crystal research. An intriguing example is given by bent-core molecules that are themselves achiral, yet build up chiral smectic (layered) phases[1]. This is in contrast to the case of standard rod-like calamitic molecules whose phase chirality requires molecular chirality. A recently introduced new design concept is to work with an intermediate shape: hockey stick-shaped molecules[2,3]. These are non-straight molecules with two terminal chains, one of which is attached in meta-position to the three- or four-ring calamitic core. Depending on the length of the terminal chains and on the type and direction of the linking groups between the aromatic rings, conventional nematic, SmA and SmC phases can be observed, but also the loss of liquid crystalline behaviour[2,4]. It is a current matter of discussion if achiral mesogens of this type can form chiral phases on their own or not[2,5].

For achiral dialkyloxy substituted hockey stick compounds with a COO and CH=N linking group between the phenyl rings, Das et al.[3] reported the interesting phase sequence SmC - SmC_a. Both these phases are smectic with the molecules tilted a certain angle θ away from the layer normal, but the tilt is in the same direction in adjacent SmC layers (synclinic tilting order), whereas it alternates in direction between layers of the SmC_a phase (anticlinic order). Symmetry requires that the transition between the phases be first order (there is no transition state possible where both phases become identical). The SmC_a phase is relatively rare, and the sequence SmC – SmC_a very much so, for mesogens having no asymmetric carbon atom[6]. Hockey stick-shaped achiral mesogens seem to be unusually capable of generating such a phase sequence, as confirmed by two other research groups. Jones et al.[7] found a sequence SmA - SmC - SmC_a for a siloxane substituted hockey-stick-shaped compound and Yu et al.[2] reported a SmC - SmC_a transition for a hockey stick mesogen containing four aromatic rings. Very recently, Yu and Yu presented a series of hockey stick mesogens containing C=C linking groups[8].

The purpose of the present study was to investigate the balance between syn- and anticlinicity in tilted smectic phases of achiral hockey-stick mesogens as a function of the length of the shape-defining *m*-substituted terminal chain, as well as upon doping with chiral mesogens of ordinary calamitic type. Two homologous series of achiral hockey stick-shaped compounds were investigated, and one member was selected as host for chiral doping experiments. All members of both achiral series exhibit the SmC as well as the SmC_a phase, whereas the two calamitic chiral dopants exhibit, in addition

to SmA, only a synclinic SmC* and only an anticlinic SmC_a* phase, respectively. (The star signifies molecular chirality.) Chiral doping is an important strategy for achieving useful liquid crystalline materials but the properties of the resulting mixture can be difficult to predict[9], the present study constituting no exception.

An important property of chiral tilted smectic phases is that they show a spontaneous polarisation $\mathbf{P_s}$ in the smectic layers because of their reduced symmetry, rendering them switchable by an electric field[10]. By means of electrooptical methods this spontaneous polarisation as well as the optical tilt angle θ can be measured, so another aspect of the work was to study θ and the magnitude of the polarization, P_s, both of which are the order parameters of the tilted phase, in the mixtures as a function of chiral dopant concentration. Due to the spontaneous polarisation a chiral synclinic SmC* phase can be rendered ferroelectric, whereas the chiral anticlinic SmC_a* phase is antiferroelectric, the alternating tilt direction implying an alternating $\mathbf{P_s}$ modulation. This difference is often used to experimentally distinguish between the two structures using either dielectric spectroscopy or studying the current response during switching[11]. This possibility is not available in case of achiral SmC and SmC_a phases, since they lack a spontaneous polarisation, and it can therefore be challenging to experimentally verify with certainty whether an achiral tilted smectic phase is syn- or anticlinic. While texture investigations in many cases can reveal the clinicity, they do not always give conclusive evidence. The method of establishing the phase diagram in mixtures with chiral syn- and anticlinic reference compounds, as described in the present paper, can be a useful alternative tool in such cases.

Results and Discussion

Achiral hockey stick mesogens

The aim of the synthetic work was to find achiral compounds exhibiting thermodynamically stable SmC – SmC_a phases at temperatures not much higher than 100 °C and with a sufficiently broad temperature range for experimental investigations. To realize this we have enlarged the mesogenic aromatic core of three-ring compounds by insertion of a carbon-carbon double bond resulting in esters of the cinnamic acid, see scheme 1:

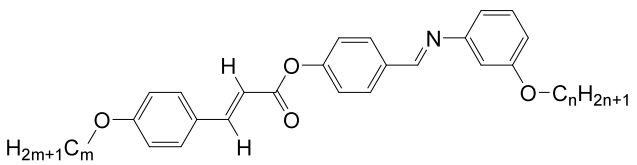

Scheme 1 General formula of the new hockey stick mesogens **m/n** (the abbreviation m/n results from the length of the two alkyloxy chains; m = 10, 12; n = 6-12, 16).

The new compounds have been prepared by condensation of 4-formylphenyl 4-n-alkyloxycinnamates with corresponding 3-n-alkyloxyanilines by refluxing in ethanol together with a catalytic amount of acetic acid. As an example the experimental procedure to prepare compound **12/8** is given together with analytical data in the experimental section.

The phase sequences of the compounds **m/n** were determined by differential scanning calorimetry (DSC), polarising optical microscopy investigations and X-ray measurements. The results are presented graphically in fig. 1 as a function of temperature and length *n* of the meta-attached alkyloxy chain. The transition temperatures and enthalpies are summarized in table 1.

Table 1 Phases, transition temperatures (°C) and transition enthalpies (kJ mol^{-1}) of the 4-(3-n-alkyloxyphenyliminomethyl)phenyl 4-n-alkyloxycinnamates **m/n**, derived from 4-n-decyloxycinnamic acid (**10/n**) and 4-n-dodecyloxycinnamic acid (**12/n**), on heating.

No. **m/n**	Cr.	SmC_a	SmC	SmA	I
10/6	81 [31.9]	101 [a]	102 [1.0]	104 [5.4]	
10/7	78 [35.7]	98 [0.11]	102 [b]	103 [4.6]	
10/8	89 [24.2]	97 [0.14]	101 [b]	102 [5.3]	
10/9	80 [40.7]	91 [0.05]	100 [b]	102 [5.2]	
10/10	77 [40.0]	92 [0.07]	99 [0.49]	100 [5.3]	
10/11	76 [40.2]	88 [c]	98 [0.21]	99 [5.1]	
10/12	77 [48.1]	88 [c]	97 [0.17]	99 [5.3]	
10/16	82 [59.5]	(80) [c]	93 [0.23]	96 [4.5]	
12/6	77 [33.6]	99 [0.32]	104 [1.9]	-	
12/7	79 [39.8]	97 [0.57]	103 [2.2]	-	
12/8	86 [46.6]	97 [0.57]	102 [1.6]	-	
12/9	84 [48.0]	93 [0.42]	102 [1.4]	-	
12/10	93 [36.9]	95 [0.48]	100 [2.7]	-	
12/11	85 [45.2]	89 [c]	99 [6.4]	-	
12/12	90 [39.8]	92 [c]	98 [6.3]	-	
12/16	83 [63.9]	87 [c]	95 [5.3]	-	

[a] In DSC the phase transitions SmC_a – SmC – SmA could not be unambiguously separated.

[b] In DSC the phase transition SmC – SmA – I could not be unambiguously separated.

[c] No transition peak could be observed for the transition SmC_a – SmC.

Characteristic polarising optical microscopy textures are shown in fig. 2, exemplified by compound **10/9** which was used as the host for the mixtures. Between ordinary glass plates, the substance had a strong tendency to align in a non-uniform way, resulting in an inconclusive texture. However, by coating the glass plates with a surfactant (cetyl trimethyl ammonium bromide; CTAB) before placing the liquid crystal upon it, a standard homeotropic alignment over the whole sample could be achieved, allowing a first classification of the phases.

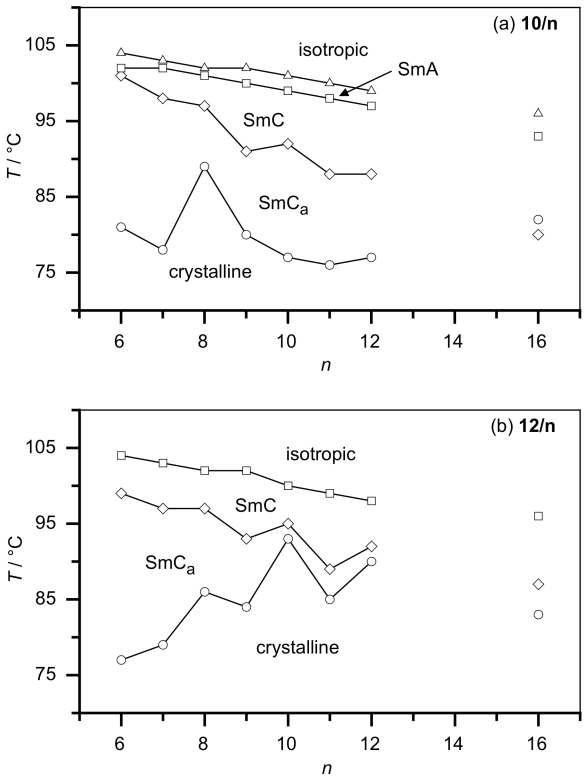

Fig. 1 Transition temperatures (on heating) of series **10/n** (a) and **12/n** (b) as a function of the length of the alkyloxy chain attached to the meta position of the terminal phenyl ring.

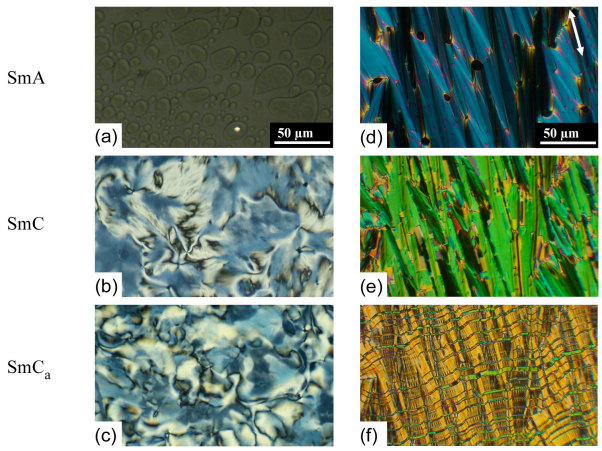

Fig. 2 Achiral host substance **10/9** on glass slides treated with surfactant (left column) and in planar-aligning cell (right column; rubbing direction indicated in *d*) at three different temperatures corresponding to the three liquid crystal phases of the compound, respectively.

The SmA phase was recognised by its complete extinction between crossed polarisers in this alignment (fig. 2a). At the transition to SmC a distinct schlieren texture suddenly developed (fig. 2b), revealing a first order transition to a SmC phase with a relatively large tilt angle θ. The transition to the anticlinic tilted phase on further cooling was easily recognised in the microscope through the appearance of strong fluctuations (fig. 2c), as typical for (chiral) SmC to SmC_a transitions[12].

Using cells in which the substrates had been coated with rubbed polyimide or nylon a relatively uniform planar alignment could be ensured. In this case the SmA and SmC phases showed typical fan-shaped textures (fig. 2d,e), the transition between the phases inducing a change in colour reflecting an increase in birefringence in SmC, as well as some splitting up into domains with opposite tilt directions. Moreover, the texture is no longer uniform in color, a result of the director adopting a lightly twisted geometry in some domains in the SmC phase, the degree of twist varying across the sample surface. The SmC-SmC_a phase transition following upon further cooling was quite striking: high-contrast stripes quickly developed parallel to the smectic layers together with a drastic colour change (fig. 2f). The latter is the result of the strong decrease in birefringence that is the consequence of the rearrangement to an anticlinic structure[13].

It should be mentioned that in both homologuous series **10/n** and **12/n** the relative temperature ranges of SmC and SmC_a, as well as the behaviour of the SmC – SmC_a clinicity transition, is clearly dependent on the length *n* of the chain attached to the meta position of the terminal phenyl ring. To rationalize these observations we point out that a lengthening of this chain can be expected to change the effective molecule shape from kinked to linear: a short chain essentially expresses the shape defined by the *m*-substitution whereas a longer chain is more flexible, allowing it to line up with the molecular long axis. Such chain length-dependent effective molecule shape in a liquid crystal phase has previously been identified for the case of mesogens with chains of varying length attached laterally to the core[14]. Looking now at fig. 1 we first note that the clinicity transition takes place deeper in the temperature range of tilted smectic order the longer the *m*-substituted alkyloxy chain, favoring SmC at the cost of SmC_a. This suggests that a well-defined kinked molecule shape (short chain) could promote anticlinic order, whereas the more rod-like shape allowed by a longer *m*-substituted chain would promote synclinic order. These observations are well in line with earlier observations of the balance between syn- and anticlinic order depending sensitively on the steric interlayer interactions, strongly influenced by the effective shape of the molecule[15].

Moroever, whereas the transition between the two tilted phases was close to immediate throughout the sample in the short-chain members, the transition process was extended over a certain temperature range (2-3 K), with different areas transitioning at different times, in the longer homologues (*n* = 12, 16). The hysteresis between heating and cooling experiments was also more pronounced the longer the *m*-substituted alkyloxy chain. To give an example the hysteresis of the SmC_a – SmC transition observed by optical studies (the transition could not be resolved in DSC due to the small transition enthalpy) amounts to about 1 K for compound 10/6 whereas it is about 5 K for the long-chain derivative 10/12. Obviously, the transition is more strongly kinetically hindered, resulting in an increased degree of supercooling/-heating, as the chain length is extended. To some extent this may be due to the larger tilt at the clinicity transition in the long-chain homologues (a result of the clinicity transition occurring at lower temperature, cf. fig. 4b), effectively

rendering the structural difference between syn- and anticlinic states greater, i.e. the phase transition requires a more extensive molecular rearrangement. The larger size of the mesogens should further enhance this effect and it also leads to an increased viscosity that may increase hysteresis effects additionally. On the other hand, the fact that the SmC – SmC_a transition enthalpy (table 1) of the n = 11, 12, 16 homologues of both series is immeasurably small shows that the thermodynamic driving force for the clinicity transition is very weak in these long homologues. The increased flexibility of the chain obviously renders the molecule compatible with syn- as well as anticlinic structure, hence supercooling/-heating effects can well be expected.

In fig. 1 one can also recognize a clear alternation tendency of the clinicity transition temperature in dependence of the number of carbon atoms in the meta-positioned chain in both series. Interestingly, it is the even-numbered alkyloxy chain members that exhibit the peaks of the alternation curve. These are the members in which the hockey stick shape is the most pronounced, hence this alternation effect again emphasizes the importance of the meta-substituted hydrocarbon chain in defining the molecule shape.

X-ray diffraction measurements on a surface-aligned sample of compound **10/10** using an area detector prove the formation of three liquid crystalline phases with layer structure on cooling. The patterns immediately below the clearing temperature (fig. 3a,d) show a 90° angle between the sharp small-angle maxima for the layer reflections (on the meridian of the pattern) and those of the outer diffuse scattering (on the equator). This is the typical pattern of a SmA phase, in which the average orientation of the main principal molecule symmetry axis is perpendicular to the layers. The layer spacing, which in SmA normally is somewhat smaller than the effective molecule length[16], amounts to 39.9 Å. Depending on the orientation of the terminal chains the molecule length can vary quite substantially (an effect of the meta-substituted alkyloxy chain), from about 34 to 43 Å (cf. fig. S1 in the ESI). The relatively large value of the layer spacing in comparison with the possible molecule lengths suggests that the most commonly adopted conformation is the one with the slightly weaker hockey stick shape.

At about 99 °C, the pattern changes, the two maxima of the outer diffuse scattering rotating out from the equator by about 14° indicating a structure with synclinically tilted molecules (SmC, fig. 3b,e). This angle increases with decreasing T to about 18° at 90°C (fig. 4b and table 1 in the ESI). In accordance with the temperature dependence of the molecule tilt, the layer spacing shrinks suddenly as a result of the SmA - SmC transition at 99°C and then decreases continuously to 37.2 Å at 90 °C (fig. 4a and table 1 in the ESI). At about 89°C, the pattern changes once more, now exhibiting broader halos for the outer diffuse scattering centred about the equator (fig. 3c,f). Their azimuthal distribution around the primary beam spot in the 2D pattern (χ distribution) may be fitted by four Gaussian curves, the four maxima yielding a tilt angle of about 19°. This pattern is in line with an anticlinic tilt of the molecules in adjacent layers (SmC_a), although it in itself is no absolute proof of this arrangement, since a synclinic structure with equally distributed domains of opposite tilt (e.g. in a sample rotationally disordered about an axis) would give the same picture. Taking the results of the other experiments into account, we can however safely conclude that the phase is SmC_a. There seems to be no significant leap in the values of the tilt angle at the SmC – SmC_a transition. On further cooling, the tilt angle in the SmC_a phase saturates at about 20°, the corresponding layer spacing being 36.8 Å (fig. 4a,b and table 1 in the ESI).

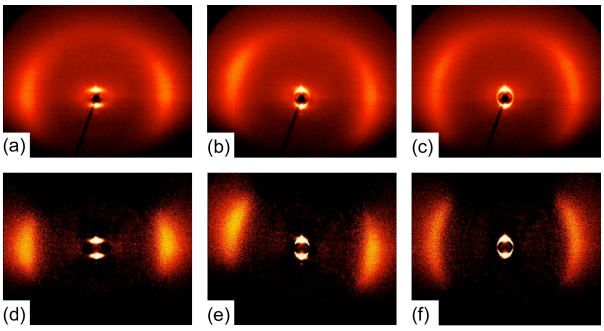

Fig. 3 2D X-ray diffraction patterns of a surface aligned sample of compound **10/10** on cooling (a to c: original patterns; d to f: scattering of the isotropic liquid subtracted to enhance the effect of the anisotropic distribution of the outer diffuse scattering): a,d) SmA phase at 100 °C, b,e) SmC phase at 95 °C with a majority of domains showing the same tilt direction (cf. fig. S2c), and c,f) SmC_a phase at 85 °C with both tilt directions equally common due to the anticlinic structure.

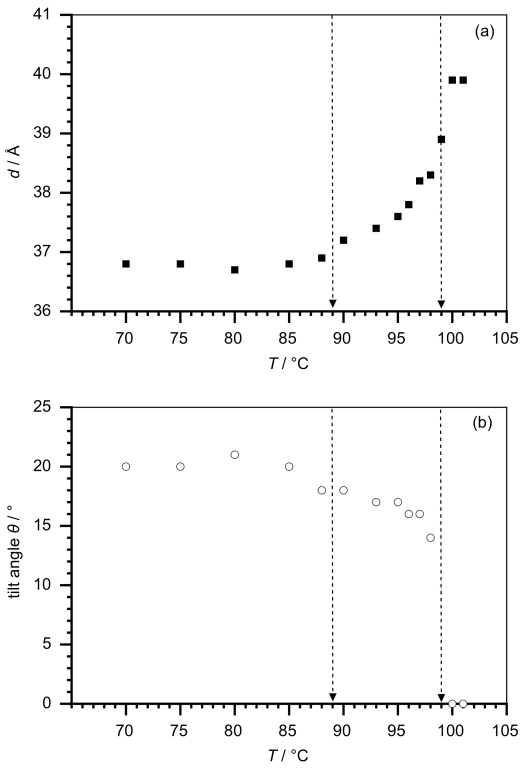

Fig. 4 Layer spacing (a) and average tilt (b) of the molecules with respect to the layer normal depending on the temperature on cooling as derived from the 2D X-ray patterns of compound **10/10** (arrows showing the approximate phase transition temperatures SmA – SmC ~ 99°C and SmC – SmC_a ~ 89°C).

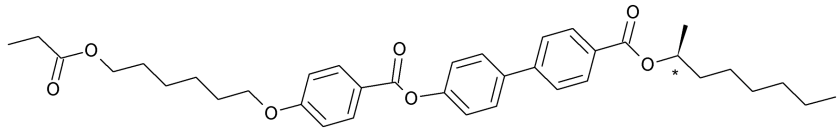

M1

chiral synclinic dopant

cryst. 56 SmC* 75.5 SmA 96.9 iso. / °C

(S)-(+)-4'-(1-methylheptyloxycarbonyl)biphenyl-4-yl 4-[(6-propanoyloxy)hex-1-oxy]benzoate

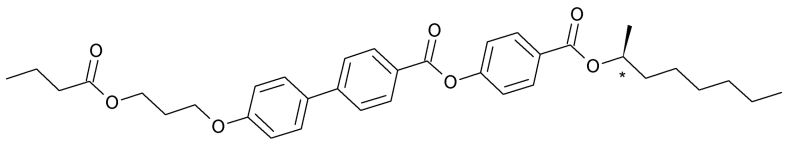

M2

chiral anticlinic dopant

cryst. 72 SmC_a* 93 SmA 117.8 iso. / °C

(S)-(+)-4'(1'-methylheptyloxycarbonyl)phenyl 4'-[(3-butanoyloxy)prop-1-oxy]biphenyl-4-carboxylate

Scheme 2 Molecular structures of the chiral compounds used for the binary mixtures and their phase sequences (on heating) as determined by DSC measurements in our laboratory.

Phase sequences of chirally doped mixtures

As the next step we studied the phase sequences of binary mixtures of the host compound **10/9** with syn- or anticlinic chiral dopants (compounds **M1** and **M2** in scheme 2). For this purpose four different methods were used: DSC, texture observations in a polarising microscope, current response measurements (yielding the magnitude of the spontaneous polarisation) and in some cases also dielectric spectroscopy. For comparison, the pure dopants were also investigated with the same methods and experimental setups, even though they have been described earlier in literature[17].

By compiling the results from these four methods the phase diagram in fig. 5 could be established. It shows the phase sequence on heating of the pure host in the middle and those of mixtures with increasing synclinic and anticlinic doping to the left and right, respectively. For some mixtures, on the syn- as well as on the anticlinic side, the temperature of the SmA*-SmC* transition detected through current response studies was somewhat higher than the transition temperature found in other ways. This can be explained by the first-order nature of the tilting transition in these mixtures. In contrast to the second-order transition case, a first order SmA*-SmC* transition can be induced by an electric field at temperatures above the zero-field transition temperature[18]. In our case, the applied field required to obtain the current response of the samples was apparently sufficient to observe this phenomenon, resulting in polarisation current peaks at temperatures where the sample in the absence of fields is in the SmA* phase. Consequently, an increased apparent transition temperature was detected.

Because the pure host shows a first and the pure dopants second order transitions one would expect a decreasing tendency towards field-induced SmC* phase with increasing dopant concentration. On the other hand, at low dopant concentrations the spontaneous polarisation is very small (see fig. 7) so that this effect in these cases could only be expected at very high electric field strengths, much higher than those applied in the current response measurements. Together these two opposing effects lead to the observation of the field-induced SmA*-SmC* transition at intermediate dopant concentrations and so explain the deviations in transition temperatures in this region of the phase diagram.

From the phase diagram it is clear that the addition of either chiral mesogen leads to a nonlinear depression of the melting point with respect to either component, while the clearing point follows an essentially linear curve connecting the clearing points of the two components (nearly constant for synclinic, continuously increasing from pure host to pure **M2** for anticlinic). These effects lead to a broader temperature range of the mesophases in the intermediate composition regimes. In both cases the temperature range of the untilted SmA phase also grows quite much, a phenomenon known from literature (see for example[16] and references therein), and it seems that even with dopant **M1** it is actually more favoured than the synclinic SmC* phase despite the dopant being of synclinic type. We also note that no intermediate smectic-C-type phases (SmC_β* and SmC_γ* [16]) appear in the phase diagram, as is sometimes the case when there is frustration between syn- and anticlinicity[19].

Focusing now on the left side of the phase diagram, we see that the synclinic doping initially does not substantially change the balance in the phase sequence. Up to around 20 mol% **M1** only a slight increase of the SmC_a* temperature range is seen, a result of a melting point depression of ~5 K. With increasing amount of dopant this melting point depression reaches its maximum between 50 and 70 mol% **M1,** yielding a melting point of ~ 45°C to be compared with 80°C in pure **10/9** and 54°C in pure **M1**. Unexpectedly, considering the clinicity of the dopant, the growth of the mesophase temperature regime leads to a further increase of the *anticlinic* SmC_a* phase range and not of that of the synclinic SmC* phase. Instead the latter phase keeps its temperature range of about 10 K, a depression of the SmC_a*-SmC*-transition with increasing amount of compound **M1** being followed by a depression of the SmA*-SmC* transition of equal magnitude until about 70 mol% **M1**. In this part of the phase diagram the SmA* phase thus grows and already at 70 mol% the same temperature for the tilting transition as in pure **M1** is found. Beyond this point, also the synclinic phase range finally grows at the expense of the anticlinic phase which disappears only at around 90 mol% **M1**.

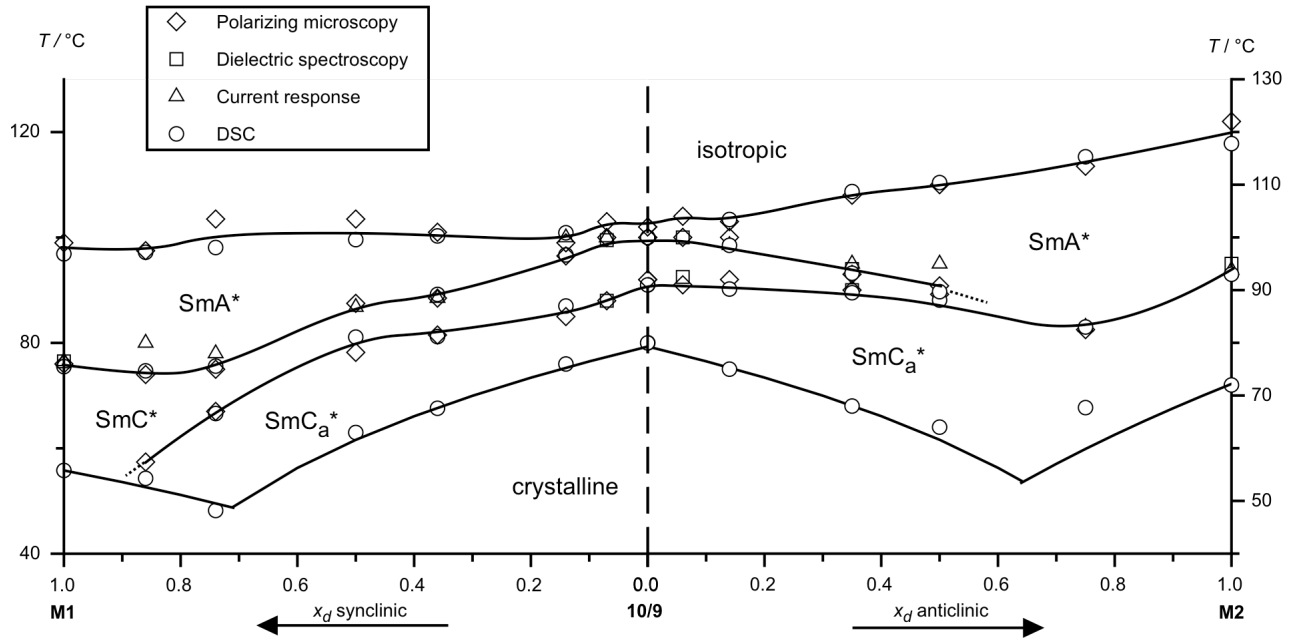

Fig. 5 Phase diagram (on heating) of mixtures between the achiral host compound **10/9** (middle) and the chiral syn- and anticlinic compounds **M1** and **M2** (towards the left and right, respectively). The melting curves on each side of the phase diagram were established by means of the Schröder-van Laar equation, in general yielding good agreement with the experimental data. The other solid lines are simply guides to the eye, biphasic regions at the first-order transitions being neglected. The crystalline regime was not further investigated.

The anticlinic mixing, shown on the right side of the phase diagram, causes a phase behaviour more similar to what might initially be expected: the synclinic phase gradually becomes smaller and disappears between 50 and 60 mol% **M2**, thus also showing a quite high stability upon addition of the anticlinic compound, although not as much as the anticlinic phase on the other side. Summarizing the observations with the two different dopants, we conclude that the influence on the clinicity balance of the type of dopant is surprisingly small. If one disregards the expansion downwards of the SmC_a* phase, which primarily is a result of the mixing-induced melting point suppression rather than an indication of enhanced tendency for anticlinic order, the balance between syn- and anticlinic order of the host compound is largely maintained up to about 40-50% dopant, the anticlinic phase being only slightly favoured.

Dielectric spectroscopy measurements[11] were consistent with the results from other techniques, cf. the example of the 35% **M2** mixture in fig. 6. For the weakly doped mixtures the results were however not very conclusive since P_s was so small that molecular fluctuation processes, rather than the more discriminative collective ones[11], dominated the spectra.

The mixture study shows that, although the temperature ranges of the syn- and anticlinic phases, respectively, of the achiral hockey stick host compound **10/9** are very similar, this compound has a somewhat stronger tendency to form the anticlinic than the synclinic tilted phase, further enhanced when mixing by a suppression of the melting point. Considering the scarcity of achiral materials forming the anticlinic SmC_a phase this suggests that hockey stick-shaped compounds of this type are interesting as components in mixtures where a broad temperature range, low-polarisation and long-pitch SmC_a* phase is desired, e. g. for antiferroelectric LCDs.

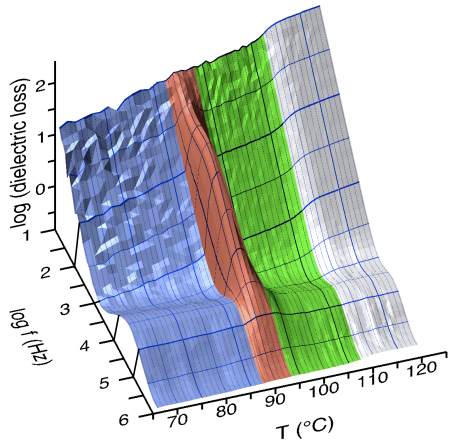

Fig. 6 Dielectric absorption spectrum of the mixture with 65% host **10/9** + 35% anticlinic chiral dopant **M2** in a 23.5 µm planar-aligned cell, obtained on cooling. Colour coding: SmC_a* = blue, SmC* = red, SmA* = green, isotropic = grey.

Order parameters of the chirally doped mixtures

In the electrooptic studies the order parameters of the tilted phases, the magnitude of the spontaneous polarisation P_s and the optical tilt angle θ (the latter only for a few mixtures), were determined, cf. fig. 7. Both pure dopants **M1** and **M2** have P_s and θ values, respectively, in the same order of magnitude (29°, 115 $nCcm^{-2}$ and 25°, 88 $nCcm^{-2}$, at a temperature of 15 K below the SmA*-SmC* and SmA*-SmC_a* transition, respectively). Because the host compound **10/9** is achiral its spontaneous polarisation is zero, rendering a reliable measurement of the tilt angle experimentally difficult.

Nevertheless, even without this value it seems that the tilt angle at a certain reduced temperature (i. e. distance from the tilting transition) in our mixtures is more or less independent of the composition for both syn- and anticlinic mixing, cf. fig. 7. We also note that the optically obtained values for the tilt angle are similar to those obtained by x-ray diffraction for the **10/10** hockey stick homologue (cf. fig. 4).

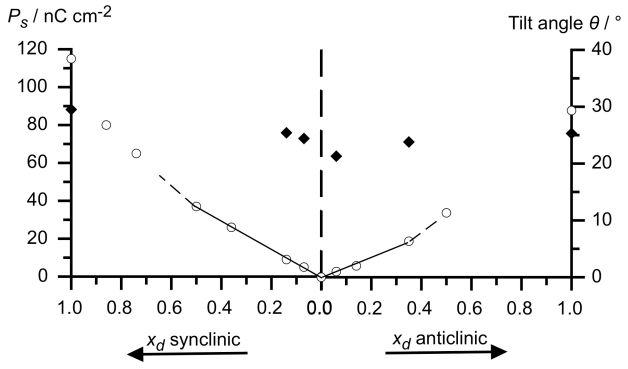

Fig. 7 Spontaneous polarisation magnitude P_s (open circles) and optical tilt angle θ (black diamonds) of the binary mixtures, in each case measured 15 K below the tilting transition, as a function of mole fraction of dopant x_d. The initial linear increase of P_s around $x_d = 0$ has been emphasized.

The spontaneous polarisation of the binary mixtures increases monotonously with increasing molar fraction x_d of chiral compound as one would expect in such an experiment, cf. fig. 7. At low concentrations a roughly linear dependency was found. From these data the polarisation power $\delta_P{}^{20}$ can be obtained, a standard measure of the efficiency of chirality transfer of each dopant:

$$\delta_P = \left(\frac{dP_0(x_d)}{dx_d} \right)_{x_d \to 0} \quad (1)$$

Here P_0 is the reduced polarisation

$$P_0 = P_S / \sin\theta \quad (2)$$

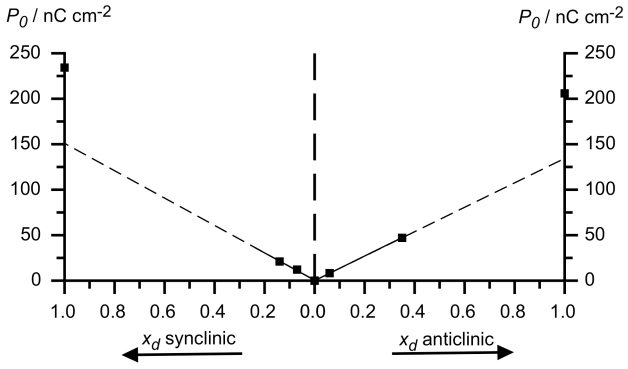

Fig. 8 Reduced polarisation P_0 as a function of molar fraction x_d of dopants showing its linear behaviour for low values of x_d.

In this way a polarisation power of 150 nCcm^{-2} for the synclinic compound **M1** and of 134 nCcm^{-2} for anticlinic compound **M2** was found, cf. fig. 8, even though due to the small number of data points this can be taken only as a rough estimation.

Conclusions

In the balance between syn- and anticlinic smectic order in hockey stick mesogens, the anticlinic structure is favored by a well-defined kinked molecule shape, achieved when the meta-substituted terminal chain is not too long. Elongation of this chain promotes the synclinic SmC phase, renders the energetic difference between SmC and SmC$_a$ very small and introduces a kinetic hinderance of the clinicity transition. By adding chiral dopants that were either strictly synclinic or strictly anticlinic to an achiral hockey stick-shaped host mesogen with roughly equal SmC and SmC$_a$ temperature ranges, we showed that the clinicity balance is significantly affected by the chiral dopant only at rather high concentration.

The synclinic SmC* phase stayed at roughly the same range in the case of a synclinic dopant whereas it suffered a small gradual decrease upon addition of an anticlinic dopant up to some 60% chiral material, i.e. well beyond typical doping concentrations. Within the same range the anticlinic SmC$_a$* phase was found to expand substantially in temperature range regardless of dopant type. The weak correlation between dopant and mixture clinicity indicates that an effective chiral dopant can be used for ferro- as well as antiferroelectric liquid crystal mixtures, even if it itself exhibits only an anticlinic or only a synclinic tilted phase, respectively. Achiral hockey stick materials like those studied here could be useful as additives in antiferroelectric liquid crystal (AFLC) mixtures in order to bring their polarization down and helical pitch up. Although there are also other obstacles to resolve before realizing commercially viable AFLC displays or other electrooptic devices, control of pitch and polarisation remain challenging but important goals when AFLC mixtures are to be tailored for application.

Experimental

Synthesis

4-(3-n-Octyloxyphenyliminomethyl)phenyl 4-n-dodecyloxy-cinnamate 12/8

0.44 g (1 mmol) 4-formylphenyl 4-n-dodecyloxycinnamate, 2.73 g (1.1 mmol) 3-n-octyloxyaniline were solved in 20 ml ethanol together with a catalytic amount of acetic acid. After refluxing the solution for 2 hours and cooling to room temperature the product was separated and crystallized twice from ethanol. White crystals. Yield 0.52 g (76%). Elemental analysis (%): calc. C 78.88, H 8.92, N 2.19; found C 78.95, H 8.92, N 2.01. ^{1}H NMR: (400 MHz, $CDCl_3$): 088 (m, 6H, CH_3), 1.25-1.48 (m, 28H, CH_2), 1.78 (m, 4H, $ArOCH_2CH_2$), 3.98 (m, 4H, $ArOCH_2$), 6.48 (d, ^3J = 16.0 Hz, 1H, ArCH=CH), 6.77 (m, 2H, ArH), 6.91 (d, ^3J = 8.9 Hz, 3H, ArH), 7.28 (d, ^3J = 8.5 Hz, 2H, ArH), 7.35 (d, ^3J = 8.5 Hz, 1H, ArH), 7.52 (d, ^3J = 8.7 Hz, 2H, ArH), 7.83 (d, ^3J = 15.8 Hz, 1H, ArCH=CH), 7.93 (d, ^3J = 8.7 Hz, 2H ArH), 8.44 (s, 1H, CH=N); ^{13}C NMR (100 MHz, $CDCl_3$): 14.18, 22.74, 22.76, 26.09,26.17, 29.25, 29.31, 29.41, 29.44, 29.63, 29.66, 29.71, 29.72, 31.89, 31.99, 68.19, 68.30, 107.18, 112.45, 112.74, 113.68, 114.10, 114.96, 122.01, 122.34, 126.57, 129.72, 129.91, 130.00, 130.08,

131.06, 133.60, 146.70, 147.18, 153.32, 158.99, 159.84, 161.42, 165.13.

Chiral compounds M1 and M2

The two chiral dopants **M1** and **M2** used in this study were synthesised in the group of Roman Dabrowski[17].

Phase characterisation

Calorimetry investigations were carried out using a Perkin Elmer Pyris 1 DSC. Texture observations of planar and homeotropically aligned samples were carried out with Olympus BH-2 or Nikon Labophot 2 polarising microscopes, the sample temperature regulated by Instec or Linkam hotstages. The first setup and one including a Jenapol Interphako (Carl Zeiss Jena) polarising microscope with an Instec hotstage were also used for the electrooptical measurements on samples in cells with thickness between 0.8 and 2.0 μm and a coating inducing planar alignment. The magnitude of the spontaneous polarisation was measured by integrating the polarisation reversal current peak while switching the sample with a triangular waveform electric field[21]. The optical tilt angle was determined by measuring the optical transmission T of both states during saturated square wave switching for several consecutive sample orientations φ. By fitting $\sin^2\varphi$ functions to the two resulting $T(\varphi)$ data sets the tilt angle is extracted from their relative phase shift[22].

X-ray investigations were performed on a small droplet of the sample on a glass plate aligned upon slow cooling at the sample–glass or at the sample–air interface. The sample was held on a temperature-controlled heating stage, which partially shadows the patterns below the equator. The diffraction patterns were recorded with a 2D detector (HI-STAR, Siemens) using Ni-filtered CuK_α radiation. Dielectric spectroscopy measurements were carried out using an HP 4192 A bridge on 23.5 μm planar-aligned samples.

Acknowledgments

Financial support from the Deutsche Forschungsgemeinschaft and the "Excellenzcluster nanostrukturierte Materialien" of the Land Sachsen-Anhalt is gratefully acknowledged.

Notes and references

[a] *Martin-Luther-University Halle-Wittenberg, Institute of Chemistry – Physical Chemistry, Muehlpforte 1, 06108 Halle, Germany. Fax: +49 (0)345 55257400; Tel: +49 (0)345 5525836; E-mail: jan.lagerwall@chemie.uni-halle.de*

[b] *University of Stuttgart, Institute of Physical Chemistry, Pfaffenwaldring 55, 70569 Stuttgart, Germany. Fax: +49 (0)711 68562569; Tel+49 (0)711 68564460; E-mail: f.giesselmann@ipc.uni-stuttgart.de*

[c] *Military University of Technology, 00-908 Warsaw, Poland. E-mail: rdabrowski@wat.edu.pl*

[§] *Currently at Centre of Molecular materials for Photonics & Electronics, Department of Engineering, University of Cambridge, UK.*

† Electronic Supplementary Information (ESI) available: optimized molecular conformations and details of the x-ray investigations. See DOI:

1 D. R. Link, G. Natale, R. Shao, J. E. Maclennan, N. A. Clark, N. E. Körblova and D. M. Walba, *Science*, 1997, **278**, 1924-1927; G. Pelzl, S. Diele and W. Weissflog, *Adv. Mat.*, 1999, **11**, 707-724; R. Amaranatha Reddy and C. Tschierske, *J. Mater. Chem*., 2006, **16**, 907-961; H. Takezoe and Y. Takanishi, *Jpn. J. Appl. Phys. 1*, 2006, **45**, 597-625.

2 F. C. Yu and L. J. Yu, *Chem. Mater.*, 2006, **18**, 5410-5420.

3 B. Das, S. Grande, W. Weissflog, A. Eremin, M. W. Schröder, G. Pelzl, S. Diele and H. Kresse, *Liq. Cryst*., 2003, **30**, 529-539.

4 M. Hird, Yann Raoul, J. W. Goodby and H. Gleeson, *Ferroelectrics*, 2004, **309**, 95-101; H. Okamoto, Y. Morita, Y. Segawa and S. Takenaka, *Mol. Cryst. Liq. Cryst.*, 2005, **439**, 221.

5 S. T. Wang, S. L. Wang, X. F. Han, Z. Q. Liu, S. Findeisen, W. Weissflog and C. C. Huang, *Liq. Cryst.*, 2005, **32**, 609-617; R. Stannarius, J. Li and W. Weissflog, *Phys. Rev. Lett.*, 2003, **90**, 025502.

6 M. Rosario de la Fuente, E. Martin, M. Angel, P. Jubindo, C. Artal, B. Ros and J. L. Serrano, *Liq. Cryst*. 2001, **28**, 151-155; J. Gasowska, R. Dabrowski, M. Filipowicz and J. Przedmojski, *Ferroelectrics*, 2006, **343**, 61-67.

7 C. D. Jones, R.-F. Shao, A. G. Rappaport, J. E. Maclennan, N. A. Clark, E. Körblova and D. M. Walba, *Liq. Cryst.*, 2006, **33**, 25-32.

8 F. C. Yu and L. J. Yu, *Liq. Cryst.*, 2008, **35**, 799-831.

9 M. P. Thompson and R. P. Lemieux, *J. Mater. Chem.*, 2007, **17**, 5068-5076; R. Lemieux, *Acc. Chem. Res*., 2001, **34**, 845-853.

10 R. B. Meyer, L. Liebert, L. Strzelecki and P. Keller, *J. de Phys. Lett.*, 1975, **36**, L69-L71.

11 J. P. F. Lagerwall and F. Giesselmann, in *Chiral Liquid Crystals*, ed. W. Kuczynski, Polish Academy of Sciences, 2005.

12 A. Chandani, E. Gorecka, Y. Ouchi, H. Takezoe and A. Fukuda, *Jpn. J. Appl. Phys. 2*, 1989, **28**, L1265-L1268.

13 S. T. Lagerwall, A. Dahlgren, P. Jägemalm, P. Rudquist, K. D'havé, H. Pauwels, R. Dabrowski and W. Drzewinski, *Adv. Funct. Mater*., 2001, **11**, 87-94.

14 W.Weissflog, *Laterally substituted and swallow-tailed liquid crystals*, in *Handbook of Liquid Crystals*, ed. D. Demus, J. Goodby, G.W. Gray, H.-W. Spiess and V. Vill, Wiley-VCH, Weinheim, 1998, vol. 2B, pp. 835-863.

15 J. Thisayukta and E. Samulski, *J. Mater. Chem*. 2004, **14**, 1554-1559; K. Kumazawa, M. Nakata, F. Araoka, Y. Takanishi, K. Ishikawa, J. Watanabe and H. Takezoe, *J. Mater. Chem*. 2004, **14**, 157-164.

16 J. P. F. Lagerwall and F. Giesselmann, *ChemPhysChem*, 2006, **7**, 20-45.

17 J. Gasowska, R. Dabrowski, W. Drzewinski, M. Filipowics, J. Przedmojski and K. Kenig, *Ferroelectrics*, 2004, **309**, 83-93; Z. Raszewski, J. Kedzierski, J. Rutkowska, W. Piercek, P. Perkowski, K. Czuprynski, R. Dabrowski, W. Drzewinski, J. Zielinski and J. Zmija, *Mol. Cryst. Liq. Cryst.*, 2001, **366**, 607-616.

18 Ch. Bahr and G. Heppke, *Mol. Cryst. Liq. Cryst*., 1987, **150B**, 313-324.

19 J. P. F. Lagerwall, F. Giesselmann, Ch. Selbmann, S. Rauch and G. Heppke, *J. Chem. Phys.*, 2005, **122**, 144906; J. P. F. Lagerwall, G. Heppke and F. Giesselmann, *Eur. Phys. J. E*, 2005, **18**, 113-121.

20 K. Siemensmeyer and H. Stegemeyer, *Chem. Phys. Lett.*, 1988, **148**, 409-412.

21 K. Miyasato, S. Abe, H. Takezoe and A. Fukuda, *Jpn. J. Appl. Phys. 2*, 1983, **22**, L661-L663.

22 C. Bahr and G. Heppke, *Liq. Cryst.*, 1987, **2**, 825-831; F. Giesselmann, A. Langhoff and P. Zugenmaier, *Liq. Cryst.*, 1997, **23**, 927-931.